

Comparative Evaluation of Speckle Tracking Methodologies in Intravascular Ultrasound Images

M.A.V.M.Grinet*, M.C. Moraes**, T. Yoneyama*

*Aeronautical Institute of Technology, São José dos Campos, SP, Brazil

**Institute of Science and Technology, Federal University of São Paulo, São José dos Campos, SP, Brazil

e-mail: mgrinet1@gmail.com, matheus.moraes@unifesp.br, takashi@ita.br

Abstract – *The aim of this study is to, first, propose a framework to evaluate speckle-tracking parameters on intravascular ultrasound imaging of arteries, and second, to propose two speckle-tracking parameters. The framework proposed utilizes a numerical phantom of the artery and artificially displaces an atherosclerotic plaque, providing a known displacement map of the plaque. We track the displacement of the plaque using five distinct speckle-tracking parameters based on a block-matching method through eight subsequential frames. The estimated displacements from the tracking parameters evaluated are compared with the known displacement through Pearson correlation. This study has the potential to provide a new metric for evaluating distinct speckle-tracking parameters and methods, contributing to provide a safer, more accurate method of evaluating atherosclerotic plaques.*

Keywords: *Speckle-tracking, Ultrasound, Atherosclerosis, IVUS, Block-matching.*

Introduction

Cardiovascular diseases (CVDs) are responsible for a major impact to the economy and to the public health in the United States of America, and in the world [1]. The impact of CVDs have in society is significant enough that the American Heart Association (AHA), in conjunction with the Center for Disease Control and Prevention (CDC) publishes annual statistical revisions in order to empower doctors, researchers, and other members of the healthcare sector with critical resources. According to Roger et al. (2012) [2], the estimated costs related to CVDs in the United States alone, in 2007 and 2008, were of U\$286 and U\$297.7 billion, respectively, which is a significantly higher cost as compared to other diseases.

Atherosclerosis (AT) is a disease of the arterial wall that occurs in susceptible areas of the main arteries. Starting with the retention of lipids, followed by oxidation, and modification that cause chronic inflammation, which can lead to

thrombosis or stenosis. AT lesions can cause thrombotic occlusions of the main arteries of the heart, brain, legs, and other organs. The lesions start on the internal arterial wall – the intima – and progressively affect the entire arterial structure, including the media and the adventitia [3]. The risk factor of AT is directly proportional to the composition and morphological aspects of the plaque accumulated on the intima. The accumulated tissue can present a calcified, fibrous, or lipidic aspect, or a combination of these [4]. The identification and characterization of this accumulated tissue is crucial for an efficient and precise clinical approach, providing insight information that assist in clinical decisions and surgical interventions [5]. In order to obtain this information, intravascular ultrasound (IVUS), a medical imaging modality crucial for cardiac interventions, is widely used [6].

IVUS imaging provides anatomical and morphological information of the coronary artery and of the accumulated plaque tissue that is fundamental for a reliable diagnosis [6, 7]. This imaging modality allows for the visualization of sections of the coronary artery, such as the lumen, intima, media, adventitia, and accumulated atherosclerotic plaques [7]. The lumen is the arterial pathway for the blood, delineated by the intima, the innermost part of the arterial wall. The media is composed of muscle cells and elastic tissue, positioned between the intima and the adventitia. The adventitia is the outermost layer of the artery, delineated by the media [6]. In order to extract relevant information that can contribute to the treatment of AT, it is necessary to obtain subsequent IVUS images from the same arterial segment under different intraluminal pressures [8], allowing for a dynamic analysis of the tissue submitted to different mechanical stresses. Through the evaluation of the mechanical behavior of the tissues, it is possible to characterize the AT plaques with basis on their mechanical properties, allowing for the identification of lipidic, fibrous, or calcified plaques and leading to a more reliable clinical intervention with higher chance of success [9].

Tracking displacement of the microstructures of interest in the imaged tissue is an important part of proper mechanical characterization. Natural acoustic markers, or speckles (small white regions visible in grayscale ultrasound imaging), represent specific patterns of the imaged tissue. Speckle-Tracking analysis (ST) identifies the speckles and tracks their displacement within the imaged section. ST is widely described in the literature within a block matching (BM) framework [10], in which a small region around a point of interest $p(x, y, k)$, denominated the block of reference B_{ref} , is selected as the pattern to be tracked throughout the different frames. In order to reduce the computational cost and to obtain improved accuracy, several authors propose a search window around B_{ref} encompassing all possible displacement locations of $p(x, y, k)$ [11-13].

The objective of the present work is to, firstly, evaluate the accuracy of BM based ST utilizing parameters from the literature [11-13] through the comparison of tracked displacements $\hat{d}(x, y)$ with known displacements $d(x, y)^{Real}$. Numerical phantoms of the artery are used in order to artificially displace AT plaques and obtain $d(x, y)^{Real}$. Secondly, two specific parameters for ST are proposed and compared to existing works in terms of yielded accuracy.

Materials and methods

Here we present the framework used for comparing the considered ST parameters. The used test images have two coordinates (x, y) within the same frame, as well as a temporal coordinate (k) between all subsequent frames.

Speckle-Tracking

First, a point $p(x, y, k)$ is selected manually in the first frame, defining the object of interest to be tracked. Centered around $p(x, y, k)$, the reference block B_{ref} with dimensions $[B_{ref-X}, B_{ref-Y}]$ is selected as the reference pattern to be tracked in the following frame, as illustrated below (Figure 1). On the subsequent frames, a search window with dimensions $[W_X, W_Y]$ automatically centers on the initial point, where W_X and W_Y are the number of reachable neighbors, delineating an area of possible displacement of the reference pattern within B_{ref} .

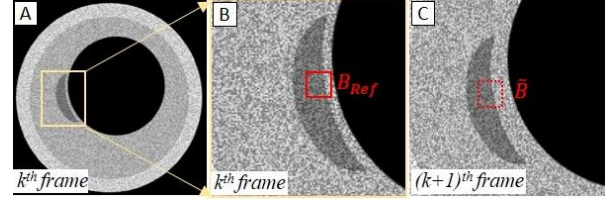


Figure 1. Initialization phase of ST. (A) Selection of starting point in numerical phantom of IVUS imaging of the arterial wall with plaque. (B) Selected reference block B_{ref} (red) within search window (yellow). (C) Candidate block \tilde{B} in the $(k+1)^{th}$ frame.

Following the selection of the reference block and the search window, the similarity of candidate blocks \tilde{B} and B_{ref} are calculated for each point location within the search window in the following frame by means of the square error criterion (MSE), as described below:

$$MSE = \frac{1}{n} \sum_{i=1}^n (\tilde{B}_i - B_{ref\ i})^2 \quad (1)$$

In this method, the candidate blocks in the $(k+1)^{th}$ frame with higher likelihood to correspond to the reference block will produce a smaller MSE, as their speckle present similarity to the reference. The presented output is the last block analyzed within the search window with the highest similarity. The position $\hat{p}(x, y, k+1)$ of the center pixel within the best \tilde{B} is stored and the process is repeated for the remaining pixels in the k^{th} frame within the search window. The displacement of each stored pixel is calculated through the difference between $\hat{p}(x, y, k+1)$ and $p(x, y, k)$, described below:

$$\hat{d}(x, y) = [\hat{p}(x, y, k+1) - p(x, y, k)] \quad (2)$$

Performance evaluation

Finally, each resulting calculated displacement is compared to the known displacement from the numerical phantom through cross-correlation, as seen in Figure 2.

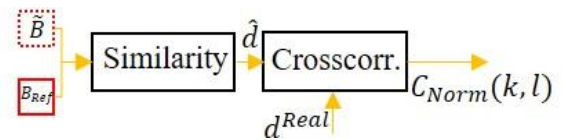


Figure 2. Block diagram representing the overall structure of the proposed ST framework.

The cross-correlation of the X-by-Y matrix of real displacements D^{Real} and the matrix of estimated displacements \hat{D} is computed by:

$$C(m, n) = \sum_{x=0}^{X-1} \sum_{y=0}^{Y-1} D^{\text{Real}}(x, y) \widehat{D}(x - m, y - n) \quad (3)$$

Where \widehat{D} is correspondent to the pixels positioned at (m, n) . We normalized the output of the cross-correlation, resulting in a single cross-correlation coefficient for the displacement between each frame, by:

$$C_{\text{Norm}}(m, n) = \frac{C(m, n)}{\sqrt{\sum (D_p^{\text{Real}} \cdot D_p^{\text{Real}}) \sum (\widehat{D} \cdot \widehat{D})}} \quad (4)$$

Where D_p^{Real} is the portion of the real displacement matrix that aligns with the selected region of estimated displacements \widehat{D} .

In order to avoid having a tracked pixel exit the search window, a buffer region was considered on the extremities of the search window. The values of the parameters $B_{\text{ref-X}}$, $B_{\text{ref-Y}}$, W_X , W_Y , and buffer windows were due to the max possible displacement for this application, and were described by the literature (parameters #3-5) [11-13], as well as proposed in the present work (parameters #1 and #2), as shown below (Table 1).

Table 1. Block, Search Window, and Buffer parameters for Speckle-Tracking

#	Size		
	Block [mm ²]	S.Win. [mm ²]	Buffer [mm ²]
1	0.12 × 0.12	1.20 × 2.80	0.28 × 0.28
2	0.20 × 0.20	1.00 × 2.00	0.12 × 0.12
3	1.50 × 0.30	2.10 × 0.90	0.50 × 0.20
4	1.60 × 1.00	2.90 × 2.30	0.65 × 0.65
5	0.10 × 0.10	0.70 × 0.70	0.30 × 0.30

Results

We compared the estimated displacements of the ST parameters evaluated to the known displacement obtained from the numerical phantom. The phantom represents a segment of the coronary artery, with an AT plaque, and added multiplicative speckle noise, with mean 0 and variance 0.04. The plaque in the phantom was displaced in the x-axis and y-axis artificially through 8 subsequent frames. We stored the movement in both axis between each frame as a gold standard of known displacement.

In order to test the robustness of the selected parameters, we selected three distinct regions of the plaque to be tracked: the center of the plaque; the border of the plaque; the corner edge of the plaque. We estimated the displacements between the first frame and the subsequent frames shown in Table 2.

Pearson correlation (ρ) of the estimated displacements between each frame and the known displacement in each axis was calculated for all distinct regions and ST parameters.

Table 2. Pearson Correlation Coefficient between estimated displacements and known displacements.

Center of Plaque						
#	Frame 3		Frame 5		Frame 8	
	ρ dX	ρ dY	ρ dX	ρ dY	ρ dX	ρ dY
1	0.831	0.904	0.918	0.899	0.904	0.909
2	0.741	0.783	0.754	0.737	0.783	0.686
3	0.396	0.476	0.418	0.035	0.476	0.067
4	0.229	0.556	0.464	0.464	0.556	0.530
5	1.000	0.899	1	1	0.899	0.869

Border of Plaque						
#	Frame 3		Frame 5		Frame 8	
	ρ dX	ρ dY	ρ dX	ρ dY	ρ dX	ρ dY
1	0.540	0.532	0.664	0.712	0.737	0.790
2	0.616	0.574	0.713	0.759	0.793	0.761
3	0.622	0.622	0.663	0.418	0.688	0.388
4	0.223	0.223	0.471	0.471	0.465	0.463
5	0.923	0.694	0.886	0.931	0.793	0.754

Corner of Plaque						
#	Frame 3		Frame 5		Frame 8	
	ρ dX	ρ dY	ρ dX	ρ dY	ρ dX	ρ dY
1	0.519	0.375	0.706	0.669	0.788	0.689
2	0.586	0.511	0.635	0.702	0.670	0.584
3	0.177	0.197	0.142	0.377	0.200	0.342
4	0	0	0.101	0.126	0.132	0.169
5	1	1	1	1	0.989	0.953

Discussion

We proposed two distinct ST parameters to assess the displacement of AT plaques within the intima-media complex of the arterial wall using IVUS imaging, as well as a comparison of the accuracy of the proposed parameters and of parameters obtained from the literature through a known displacement obtained from a numerical phantom.

The selection of distinct tracking regions indicated the variability in accuracy of some of the parameters.

Our proposed parameters showed promising results by accurately tracking the displacement of the center of the plaque. The small block size and large search window made it possible to track the pixel displacement as far as eight frames away, up to the 90th percentile.

Parameters 3 and 4, proposed by Zhand et al (2013), and Gastounioti et al (2011), respectively, did not perform well in our proposed trials. With a large block size, the tracking of small

displacements reached only up to the 62nd percentile for parameter 3, and 55th percentile for parameter 4

Parameter 5, proposed by Cinthio et al. (2006) showed acceptable performance in every proposed trial. This can be noted due to the parameter's small block and search window size, limiting the number of reachable neighbors that are more likely to match the reference block.

Larger block sizes have shown to be less accurate for ST in IVUS imaging. However, small block dimensions such as the ones proposed can lead to higher noise sensitivity when applied to real clinical images. In addition, we tested the parameters on an undeformable numerical phantom, and moving tissues can undergo shearing deformation during the cardiac cycle. Therefore, the real corresponding block may vary slightly from the reference block. As this work is part of an ongoing Master's thesis project, we will tackle these issues in future iterations, with a more realistic, deformable numerical phantom of the plaque and artery.

In conclusion, the use of numerical phantoms as a method for evaluating ST parameters could serve as a gold standard and guide new methods for AT plaque characterization in IVUS imaging. The results of this project will be available to the public along with the Master dissertation thesis in the future.

Acknowledgements

We would like to thank Laboratório de Processamento de Imagens Biomédicas (LABPIB) from the Institute of Science and Technology, Federal University of São Paulo, as well as the Control Systems division of the Electronics & Computer Engineering Department at Instituto Tecnológico de Aeronáutica (ITA). Finally, we would like to thank Conselho Nacional de Desenvolvimento Científico e Tecnológico (CNPq) for the financial support.

References

[1] Mozaffarian D., et al. Heart Disease And Stroke Statistics-2016 Update: A Report From The American Heart Association.; American Heart Association Statistics Committee; Stroke Statistics Subcommittee. *Circulation*. 2016, Jan, 26, 133(4):e38-360.
[2] Roger V1, et al. Executive Summary: Heart Disease And Stroke Statistics - 2012 Update: A Report From The American Heart Association. 2012; 125(1):188-97

[3] Insull Jr, W. The Pathology of Atherosclerosis: Plaque Development and Plaque Responses to Medical Treatment; *Am. J. Med.* 2009, Jan, 122(1 Suppl):S3-S14.
[4] Davies M.J. The Pathophysiology of Acute Coronary Syndromes. *Heart*. 2000; 83:361–366.
[5] Fisher A., Gustein D.E., Fayad Z.A., Fuster, V. Predicting Plaque Rupture: Enhancing Diagnosis and Clinical Decision-Making in Coronary Artery Disease. *Vascular Medicine*. 2000, 5:163-72.
[6] Papadogiorgaki M., Mezaris V., Chatzizisis Y.S., Giannoglou G.D., Kompatsiaris I. Image Analysis Techniques for Automated IVUS Contour Detection. *Ultrasound Med. Biol.* 2008, 34:1482–1498.
[7] Taki A., Hetterich H., Roodaki A., Setarehdan S., Unal G., Rieber J., Navab N., König A. A New Approach for Improving Coronary Plaque Component Analysis Based on Intravascular Ultrasound Images. *Ultrasound Med. Biol.* 2010, 36:1245–1258.
[8] Korte C.L., Steen A.F.W. Intravascular Ultrasound Elastography: An Overview. *Ultrasonics*. 2002, 40:859–865.
[9] Céspedes E.I., Ophir J., Ponnekanti H., Maklad N. Elastography: Elasticity Imaging Using Ultrasound with Application to Muscle and Breast in Vivo. *Ultrasonic Imaging*. 1993, 15(2):73-88.
[10] Bohs L., Trahey G., A Novel Method for Angle Independent Ultrasonic Imaging of Blood Flow and Tissue Motion. *IEEE Transactions On Biomedical Engineering*. 2011, 38, 280-286.
[11] Zhand G., Orkisz M., Sérusclat A., Moulin P., Vray D. Evaluation of a Kalman-Based Block Matching Method to Assess the Bi-Dimensional Motion of the Carotid Artery Wall in B-Mode Ultrasound Sequences. *Med. Image Anal.* 2013, Jul, 17(5):573-85.
[12] Cinthio M., Ahlgren A., Bergkvist J., Jansson T., Persson H., Lindstrom K. Longitudinal Movements and Resulting Shear Strain of the Arterial Wall. *Am. J. of Physiology*. 2006, 291, H394-H402.
[13] Gastouniotti A., Golemati S., Stoitsis J., Nikita K. Comparison of Kalman Filter-Based Approaches for Block Matching in Arterial Wall Motion Analysis from B-Mode Ultrasound. *Measurement Science and Technology*. 2011, 22, 14008.1-114008.9.